

Images of Nanobubbles on Hydrophobic Surfaces and Their Interactions

James W. G. Tyrrell and Phil Attard

Ian Wark Research Institute, University of South Australia, Mawson Lakes SA 5095 Australia

(Received 17 July 2001; published 8 October 2001)

Imaging of hydrophobic surfaces in water with tapping mode atomic force microscopy reveals them to be covered with soft domains, apparently nanobubbles, that are close packed and irregular in cross section, have a radius of curvature of the order of 100 nm, and a height above the substrate of 20–30 nm. Complementary force measurements show features seen in previous measurements of the long-range hydrophobic attraction, including a jump into a soft contact and a prejump repulsion. The distance of the jump is correlated with the height of the images. The morphology of the nanobubbles and the time scale for their formation suggest the origin of their stability.

DOI: 10.1103/PhysRevLett.87.176104

PACS numbers: 68.15.+e, 68.37.Ps

The long-ranged (10–100 nm) attraction measured between macroscopic hydrophobic surfaces (see Ref. [1] and references therein) has stimulated wide-ranging debate on the origins and implications of the phenomenon. One proposal, that the attraction is due to preexisting bubbles that bridge the two approaching hydrophobic surfaces [1,2], is gaining increasing acceptance. The idea is supported by experiments that show that the force tends to be weaker and less long ranged in deaerated water [3,4], and it has received some recent impetus from colloid probe force measurements [5], which show unique features implicating nanobubbles, whose size is deduced from the range of the attraction. Thermodynamic calculations have quantified the details of the force due to bridging nanobubbles [6], and the colloid probe force measurements have been replicated by a number of authors who reach similar conclusions [7–10].

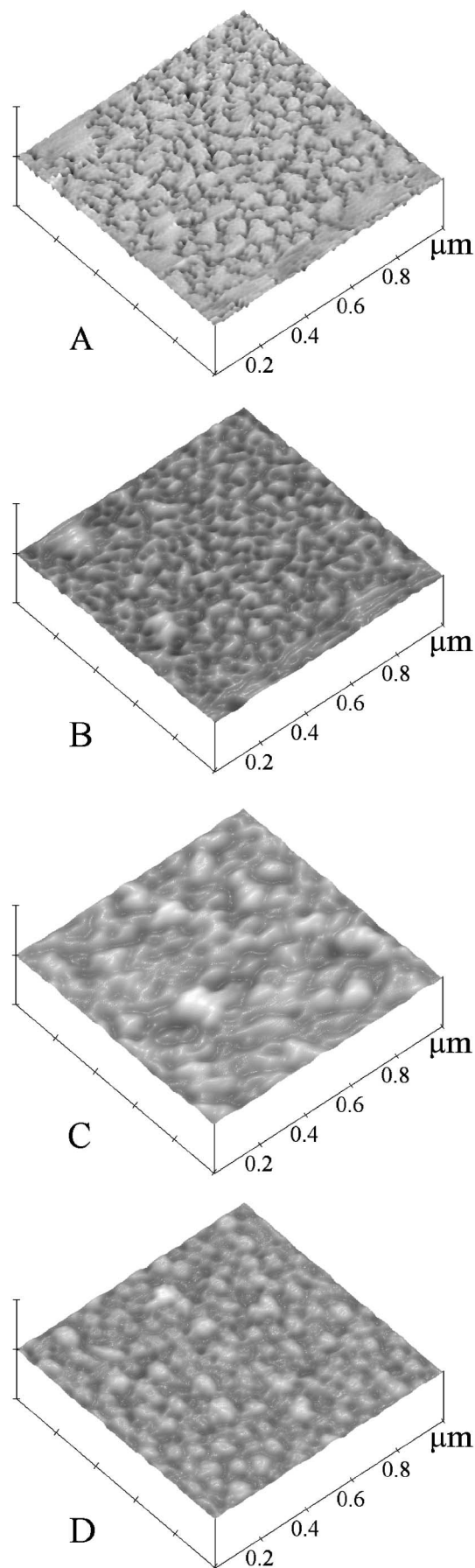
Despite this emerging consensus there remain difficulties with the idea. It is hard to reconcile the existence and apparent stability of nanobubbles with conventional thermodynamics. They should rapidly dissolve because their high internal gas pressure precludes equilibrium with the atmosphere, a significant problem that was noted by the original proponents of the theory [1,2]. Moreover, the evidence for nanobubbles is necessarily indirect; their presence is deduced from the features of the force measurements and other possibilities cannot be excluded. The putative size of the bubbles is less than the wavelength of light, which rules out optical observation.

Here direct visual evidence is obtained for nanobubbles by imaging hydrophobic surfaces in water using scanning probe microscopy in the tapping mode. The more common contact mode imaging destroys or displaces the nanobubbles, which are apparently very delicate. The nanobubbles cover the surfaces, and striking pictures of their size and shape are obtained. The correlation of the features of the images with consecutive force measurements adds to the evidence implicating nanobubbles as the origin of the long-range hydrophobic attraction. The morphology of the

bubbles and their evolution in time to some extent accounts for their thermodynamic stability.

Glass surfaces were washed, dried in a clean room environment, and exposed to dichlorodimethylsilane vapor for 3 min [8], which gave a measured advancing contact angle of 101°. Purified water (Elga UHQ), with *pH* 5.6 after exposure to the atmosphere, was used, and drops of KOH or HNO₃ were added to give the desired *pH*. Tapping mode images were acquired with a Nanoscope IIIa (Digital Instruments) using a fluid cell and a bare Si₃N₄ cantilever (0.38 N/m) at frequencies of 8.4 kHz and a scan speed of 4 μm/s. A drive amplitude of 230 mV was used, which from amplitude versus distance plots corresponded to free peak-to-peak cantilever oscillations of around 2.5 μm. The images were very sensitive to the drive amplitude and were severely degraded by as little as a 5% change either way. Fourier filtering was applied to the images to remove high frequency noise. For the force measurements a silica sphere (Geltech, 7.5 μm diam) was attached as received to a cantilever (0.58 N/m) and briefly (30 s) exposed to the silane vapor. The contact angle could not be measured directly, but subsequent pull-off force measurements were consistent with a capillary adhesion for a contact angle of 80°. The images and force curves presented below are a representative selection of those analyzed in the course of these experiments.

The images of the hydrophobic surfaces in Fig. 1 show quite marked domains or features, which are henceforth referred to as nanobubbles. The rationale for this is the large phase shifts in Fig. 1(A), which indicate that the corresponding features in Fig. 1(B) are composed of much softer material than the substrate, and that it is not simply surface roughness that is being imaged. Indeed, contact mode imaging in air and in water revealed smooth featureless surfaces with a root mean square roughness of less than 0.5 nm. The nanobubbles were somewhat ephemeral and were easily destroyed by using a larger drive amplitude or by using the contact mode (see below). The images show that the surfaces are covered by an irregular network



of nanobubbles, and that they are, if not contiguous, at least close packed [11]. Analysis of the image shows the individual nanobubbles to have a mean height 20–30 nm, and mean area $4\text{--}6 \times 10^3 \text{ nm}^2$, which increases with decreasing pH . (The area is somewhat dependent on the threshold chosen for the domain decomposition.) At high pH the air-water interface is negatively charged, and the mutual repulsion of the bubbles may account for their more regular shape. No discernable change in morphology or distribution of the bubbles was observed over the several hours of a series of experiments.

Figure 2 shows force curves between the silica colloid and the hydrophobic substrate. The jump into contact seen here arises when the gradient of the attractive force exceeds the cantilever spring constant, and it signifies the bridging of a nanobubble between the two surfaces [1,5]. The separation at which the jump occurs is close to the height of the nanobubbles in Fig. 1. The attraction arises because it is favorable to replace the costly liquid-vapor interface by a solid-vapor interface, and once bridging has occurred the bubble grows laterally. The soft contact or hook region following the jump (inset) has been interpreted as a dynamic effect due to this lateral spreading [5,6]. Calculations predict that the minimum decreases and the width increases with increased driving velocity due to the decreased equilibration time [6], a prediction which the results in Fig. 2 support. Prior to the jump there is a long-range repulsion, as has also been observed previously [5,7]. When artifacts due to laser interference are removed, this repulsion is found to be almost independent of pH and driving velocity and to have a decay length of 25 nm, which is much shorter than the Debye length. The velocity dependence in Fig. 2 also shows that the separation at which the jump occurs decreases with increasing drive velocity. In so far as the jump represents an instability, this is consistent with the notion that a critical fluctuation in the interface is more likely to occur at a larger separation for a slow-moving probe than a fast-moving one because of the longer time it takes to approach.

From the jump-out distance of the retract force in Fig. 2 it is possible to estimate the adhesion as 64–102 nN. This is consistent with a capillary adhesion for a bubble between a flat and a sphere with contact angles of 101° and $80^\circ\text{--}82^\circ$, respectively (calculated in the bridging cylinder approximation [6]). A new feature evident in the retract force following the jump out of contact is the flat, weak attraction and the multiple steps. At large separations bridging bubbles of submicroscopic size are stable with respect to microscopic ones, and conversely at contact, and the attraction due to the former is weak and slowly varying [6]. The data therefore indicate that during the jump out of contact

FIG. 1. AFM tapping mode images of a $1 \mu\text{m}$ square of the hydrophobic glass surface in water. The peak-to-trough scale is 10° in the phase image (A) and 30 nm in the height images (B)–(D). The pH is 5.6 [(A) and the corresponding height image (B)], 3.0 (C), and 9.4 (D).

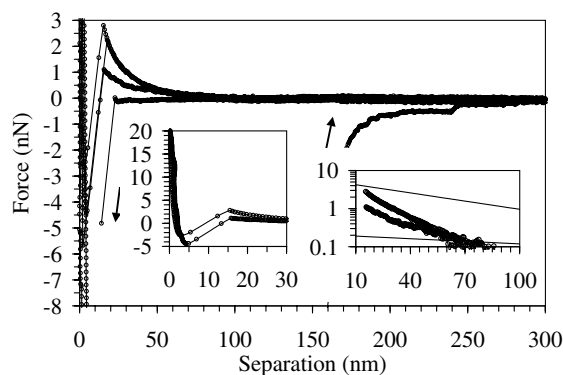


FIG. 2. Approach and retract force curves between the hydrophobic surface and the silica sphere. Taking the maxima prior to jump in as a reference, the curves correspond to (from top to bottom) pH 9.4, 9.4, 5.6, and 3.0 and velocity 13.8, 0.4, 6.9, and 0.2 $\mu\text{m/s}$, respectively. The retract curve is for the pH 5.6, 6.9 $\mu\text{m/s}$ case. Note the weak, slowly varying attraction and multiple steps at large separations. Left inset: approach curves for pH 5.6, 6.9 $\mu\text{m/s}$ and pH 9.4, 13.8 $\mu\text{m/s}$ detailing the postjump soft contact. Right inset: logarithm of the prejump repulsion. The top curves correspond to pH 9.4, 0.4, and 13.8 $\mu\text{m/s}$, and the bottom curve corresponds to pH 5.6, 6.9 $\mu\text{m/s}$. The lines have arbitrary magnitude and slope equal to the Debye length.

the microscopic bridging bubble collapses to the submicroscopic branch and that this collapse is sufficiently violent and rapid that multiple submicroscopic bubbles bridge the surfaces, with the steps on each force indicating the sequential snapping of each strand.

As mentioned above, contact mode imaging of the hydrophobic surface in water was featureless and showed no nanobubbles. Working on the hypothesis that in the contact mode the tip presses so hard that it sweeps the nanobubbles aside, an attempt was made to elucidate the time evolution of the nanobubbles by seeing how long they would take to reassemble on the surface, if at all. Immediately following a contact mode image on a 1 μm square, which showed no features, a tapping mode image was made on an encompassing 3 μm square (Fig. 3). Close inspection reveals the outline of the contact mode area in the right-hand corner of the image. The three large features next to the contact square exhibit little phase change from the substrate (not shown) and are possibly tip debris from the contact mode imaging. For all intents and purposes the nanobubbles have reemerged within the 10–20 min it took to perform the second image. This strongly suggests that the hydrophobic surface is acting as a nucleation site for air in effectively supersaturated water. (It is also possible that the nanobubbles are laterally mobile on the surface and that the original bubbles that were swept aside have returned.)

In conclusion, the images coupled with force curves provide powerful evidence of the existence of nanobubbles and of their bridging as the cause of the long-range attractions measured between macroscopic hydrophobic surfaces. The evidence that the features appearing in the images are indeed nanobubbles is their phase difference,

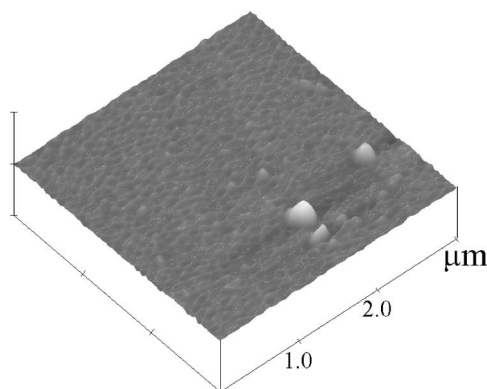


FIG. 3. AFM tapping mode image at pH 5.6 immediately following (≈ 10 – 20 min) a featureless contact mode image also in water on a 1 μm square in the right-hand corner of the picture, centered at about (2 μm , 0.8 μm). The height scale is the same as in Fig. 1, but the lateral extent is 3 times larger.

which indicate that they are softer than the substrate, their susceptibility to complete destruction by pressing too hard, and their reemergence or self-generation over time. The detailed features of the force curves on approach have previously been interpreted in terms of nanobubbles [1,5,6]. The images presented here support the view that the distance of the jump in to contact is comparable to the height of the nanobubbles above the substrate. The packing density of the nanobubbles compared to the size of the colloid probe suggests that the measured force is due to many rather than one nanobubble, contrary to speculation based upon the force curves alone [5]. Two new pieces of evidence from the retract curves may also be added. First, the measured adhesion is consistent with a capillary adhesion for two surfaces with the expected contact angles. Second, the steps and slowly varying weak attraction after the jump out of contact are consistent with the thermodynamic calculation that there is a transition from microscopic to submicroscopic bridging bubbles [6].

The images presented here go a long way to resolving the paradox of nanobubbles. The long-standing difficulty has been that the Laplace equation predicts that nanoscopic bubbles should have a very high internal gas pressure (a 10 nm nanobubble would have a pressure of 140 atm). In other words, the air in the nanobubble cannot be in equilibrium with the atmosphere and the bubble should rapidly dissolve [1,2,12]. Underlying this argument has been the implicit assumption that the jump-in distance (10–30 nm) represents the radius of curvature of the nanobubbles. The images presented here show that this is not the case and that the lateral extent of the nanobubbles is very much greater than their height. In other words, the bubbles are pancake shaped and rather flat, and the internal gas pressure is therefore much less than previously believed. The irregular and noncircular shape of the nanobubbles indicates that the driving force to minimize the area of the liquid-vapor interface is small compared to the forces that pin the contact line to the substrate. Further, the rapid reemergence of the nanobubbles after they are swept aside suggests that the

hydrophobic surface is acting as a nucleation site and that the water is supersaturated with air (due possibly to heating by the laser, the entrainment of microscopic bubbles during solution exchange, and the limited access to the atmosphere from the closed fluid cell).

The images of hydrophobic surfaces presented here reveal one further surprise. The nanobubbles do not occur in isolation with small surface coverage. They literally cover the surface, and it is difficult to see the bare substrate anywhere. One of the most interesting consequences of this picture is for the flow of water next to a hydrophobic surface, or in a hydrophobed capillary, or for the movement of a hydrophobic particle through water. The images suggest that the stick boundary conditions traditionally assumed in hydrodynamics are inapplicable for hydrophobic surfaces, and it would be more appropriate to invoke the slip boundary conditions of a fluid interface, as indeed the experimental record indicates (see Refs. [13,14] and references therein).

We thank Kristen Bremmell for suggesting the experiment described in Fig. 3 and Anthony Quinn for the contact angle measurements. The financial support of the Australian Research Council through the Special Research Centre for Particle and Material Interfaces at the Ian Wark Research Institute is acknowledged.

- [1] J.L. Parker, P.M. Claesson, and P. Attard, *J. Phys. Chem.* **98**, 8468 (1994).
- [2] P. Attard, *Langmuir* **12**, 1693 (1996).
- [3] L. Meagher and V.S.J. Craig, *Langmuir* **10**, 2736 (1994).
- [4] J. Wood and R. Sharma, *Langmuir* **11**, 4797 (1995).
- [5] A. Carambassis, L. C. Jonker, P. Attard, and M. W. Rutland, *Phys. Rev. Lett.* **80**, 5357 (1998).
- [6] P. Attard, *Langmuir* **16**, 4455 (2000).
- [7] R. F. Considine, R. A. Hayes, and R. G. Horn, *Langmuir* **15**, 1657 (1999).
- [8] J. Mahnke, J. Stearnes, R. A. Hayes, D. Fornasiero, and J. Ralston, *Phys. Chem. Chem. Phys.* **1**, 2793 (1999).
- [9] N. Ishida, M. Sakamoto, M. Miyahara, and K. Higashitani, *Langmuir* **16**, 5681 (2000).
- [10] G. E. Yakubov, H. J. Butt, and O. I. Vinogradova, *J. Phys. Chem. B* **104**, 3407 (2000).
- [11] The morphology and distribution of the nanobubbles found here are qualitatively different from those found by N. Ishida, T. Inoue, M. Miyahara, and K. Higashitani, *Langmuir* **16**, 6377 (2000). Those authors observed few, isolated, nearly uniform circular objects about $0.5\text{--}1\ \mu\text{m}$ in diameter and apparently aligned. Details of the tapping mode protocol used in that study are not given.
- [12] S. Ljunggren and J. C. Eriksson, *Colloids Surf. A* **129–130**, 151 (1997).
- [13] T. D. Blake, *Colloids Surf.* **47**, 135 (1990).
- [14] O. I. Vinogradova, *Langmuir* **12**, 5963 (1996).